The Influence of Process Variation on a Cortical Bone Interference Fit Pin Connection

Nathan A. Mauntler

Tony L. Schmitz

Department of Mechanical and Aerospace Engineering,
University of Florida,
Gainesville, FL 32611

John C. Ziegert
Department of Mechanical Engineering,
Clemson University,
Clemson, SC 29607

The interference fit is a common method for creating mechanical assemblies. When manufacturing the individual components to be assembled in this method, close dimensional control of the mating components is required in order to ensure that the amount of interference is sufficient to create a secure assembly, but not so great as to cause excessive stresses or failure of the individual components. In this work, we study interference fit connections in an assembly of human (cadaveric) cortical and cancellous bone, i.e., an allograft, used in spinal fusion surgeries. A difficulty encountered in this application is that, in addition to the machining steps, the assembly must go through subsequent sterilization and lyophilization, or freeze drying, processes that may affect the quality of the interference fit. This report examines the quality of the allograft interference fits using dimensional measurements of manufactured components at all stages of the manufacturing process, followed by examination for cracking and measurement of the pull-apart forces for assemblies. The experimental results are compared to finite element models of the interference fit and also to Monte Carlo models of the assembly using a simple thick-wall cylinder model. Experimental results show that the lyophilization process significantly affects the component dimensions, resulting in a much greater spread in interference values and likely leading to cracking and/or loss of interference.
[DOI: 10.1115/1.2896103]

1 Introduction

Assemblies of human (cadaveric) cortical and cancellous bone, or allografts, are used as implants in cervical spinal fusion surgeries where two vertebrae are joined in order to replace damaged tissue or otherwise alleviate instability of the spine. Fusion is accomplished by inserting a graft, which serves as a medium through which the vertebrae can grow together, between the two vertebrae (see Fig. 1) [1,2]. In one such commercial allograft, two cortical bone plates provide structural support while a demineralized cancellous bone block enables rapid growth through the graft. The cortical plates and cancellous block are held together by two cortical interference pins, as shown in Fig. 2.

The success of this interference fit depends on the manufacturing tolerances of the components, the quality of the donor bone used to produce the graft, and the influence of additional manufacturing processes. Excessive diametric interference or brittle tissue can result in graft fracture. Conversely, insufficient interference or tissue stiffness can compromise assembly strength and result in pull-apart failure during quality assurance testing. Either scenario results in the part being scrapped at a loss to the manufacturer.

The goal of this study is to characterize the process variation in the procedures used to manufacture the allograft in order to better understand and predict failures in the interference fit connection. The paper is divided into four sections: dimensional measurements of the interference fit component diameters, mechanical testing of the interference fit strength, finite element analysis of the graft, and Monte Carlo simulation based on an analytical interference fit model. In each step, only the cortical bone components are considered (the cancellous bone serves as a growth medium and does not provide structural support).

2 Dimensional Measurements of the Interference Fit Components

Dimensional measurements of the interference fit components were performed using a three-axis coordinate measuring machine (CMM) outfitted with a touch-trigger probe. For each of ten different donors, 12 pins, 12 cortical plates, and six cancellous blocks were produced by the manufacturer, i.e., components required to manufacture six grafts. Following machining, the diameter of each pin and plate hole were measured on the CMM. From the six sets of measured parts from each donor, three were returned to the manufacturer for assembly and eventual use in pull-apart testing (Sec. 3). The remaining parts were left unassembled and were subjected to the same sterilization and preservation processes as the assembled grafts. In order to characterize the effects of each production step on the component dimensions, diametric measurements of the loose cortical pieces were repeated after chemical sterilization, lyophilization (freeze drying), and a 30 s hydration (this step is typically completed just prior to allograft insertion by the surgeon).

Cortical pin diameters were measured in the cortical plate contact regions while clamped in a manual collet holder (Fig. 3(*a*)). Following the machining portion of the production cycle, cortical plate hole diameters were measured at four locations per hole in the fixture in which they were machined (Fig. 3(*b*)). Cortical plates from indexing wheel locations 4–6 (see Fig. 4) were then removed from the machining fixture and remeasured while clamped to the CMM table (Fig. 3(*c*)).

Cortical-cancellous stack ups in Locations 1–3 of the indexing wheel were retained for assembly along with six cortical pins (two pins for each allograft). The pins were sorted so that the largest and smallest diameters for the selected donor were included in this set. The smallest pins were paired with the largest holes (and vice versa) in an effort to increase the likelihood of interference fit failures. The assembled allografts then followed the remaining steps in the production cycle including chemical sterilization and lyophilization (the 30 s hydration step was also incorporated for our measurement study). As noted previously, measurements of the remaining loose pins and plates were repeated after sterilization, lyophilization, and hydration.

Following part measurements, the predicted interference value was calculated as the difference between the average pin and hole diameters for a given donor. Box plots of the diametric interference values for each process step are shown in Fig. 5. During the manufacturer's production cycle, loose pins are bin sorted by diameter and paired with hole reamer sizes such that 25–38 μm of interference will be present; this is identified by the shaded region in Fig. 5.

The interference data suggest that lyophilization introduces the largest process variation (i.e., largest data spread) as well as a significant interference reduction (average 21 μm). Subsequent rehydration saw an increase in the mean interference by an average of 7 μm but did not reduce the spread of data.

Contributed by the Manufacturing Engineering Division of ASME for publication in the JOURNAL OF MANUFACTURING SCIENCE AND ENGINEERING. Manuscript received December 15, 2006; final manuscript received December 31, 2007; published online March 24, 2008. Review conducted by Albert J. Shih.

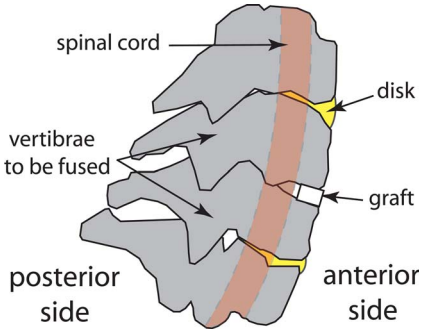

Fig. 1 Schematic of a graft inserted between vertebrae in a cervical spinal fusion surgery

Conversely, the least process variation is seen following the chemical sterilization. It is our assertion that the chemical sterilization process removed debris from the machining process from the holes. This was observed visually in many instances, although it was not possible to quantify the amount of debris removed. Due to the smaller influence of debris on hole measurements, the scatter of the data was reduced.

It should be noted that following removal from the manufacturer's machining fixture, the mean size of the cortical plate holes was found to decrease by an average of 6 μm but with a standard deviation of 7 μm. Additionally, it was noted that the standard deviations for data within a given donor was not significantly affected by the various process steps.

3 Mechanical Testing

The quality of the interference fit of the assembled allografts was evaluated by both manual and mechanical means. Prior to any mechanized testing, an attempt was made to separate the lyophilized grafts by hand. To accomplish this, each cortical plate was held between the thumb and index finger of one hand and tension was applied by the other hand. This procedure was similar to that used by the manufacturer during quality control procedures. If any resistance was met, tension was ceased. Grafts that separated with no appreciable resistance were reassembled by hand and retested as described in the following paragraphs. It should be noted that in the manufacturing environment, any graft that is separated by hand is scrapped at a loss to the manufacturer.

Of the 30 assembled grafts considered in this portion of the study, 4 (13%) failed during manual testing and 17 (57%) exhibited visible cracking in one or both cortical plates. None of the grafts that failed the manual pull-apart test corresponded to the deliberately mismatched pin/plate combinations (e.g., small pin/large plate hole). All of the cracks were in the longitudinal bone direction and ran from one or both pins to the edge of the plate or the second pin (Fig. 6).

Following manual testing, the grafts were hydrated for 30 s and mechanical pull-apart tests were carried out using an MTS Q-Test

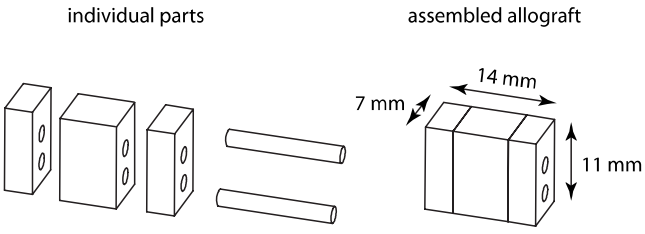

Fig. 2 Schematic of the cortical-cancellous bone allograft examined in this study. The outer cortical bone plates and inner cancellous block are joined using two cortical bone pins.

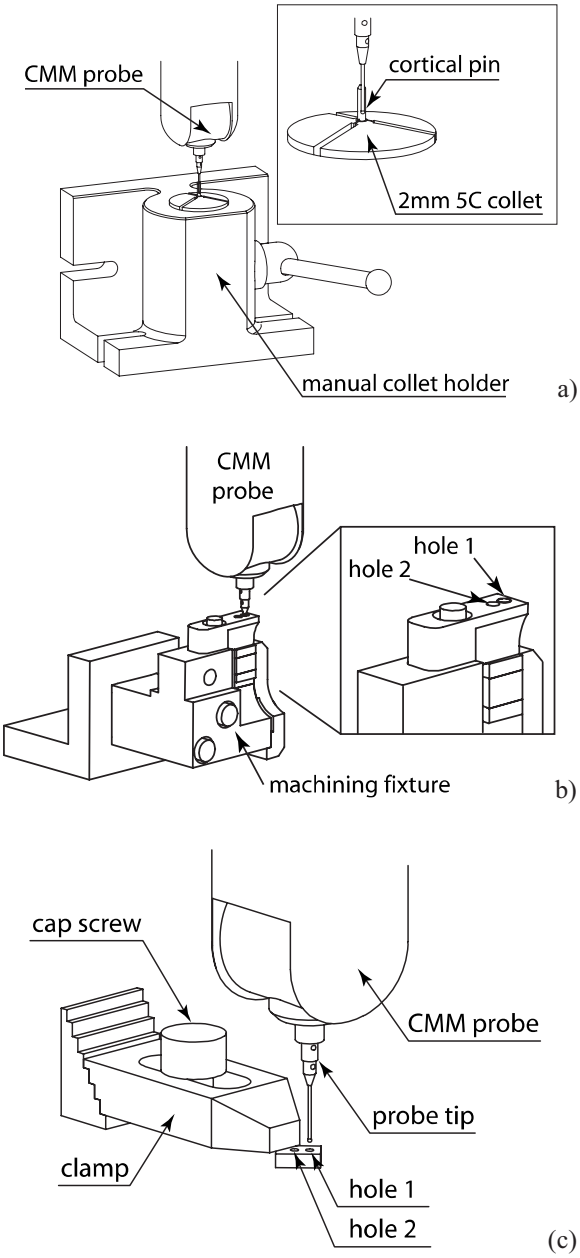

Fig. 3 Part measurements on the CMM: (*a*) cortical pins, (*b*) cortical plates held in the manufacturer's machining fixture, and (*c*) loose cortical plates

5 load frame with TESTWORKS 4 software. The load frame was fitted with a 5 kN load cell and mechanical grips, as shown in Fig. 7. The grafts to be tested were fixed with epoxy to grooved aluminum blocks, which were clamped in the mechanical grips. This approach was selected to avoid directly clamping the cortical plates, which could affect the interference connection. The 3.2 mm wide grooves in the aluminum blocks prevented the pins from being glued to the aluminum or the cortical plates, which, again, could influence the connection strength.

When the allograft-aluminum assembly was fixed in the grips, the tensile load was increased at a nominal rate of 20 N/s until the crosshead had moved by 3.5 mm, indicating that the graft had separated or broken free from either of the aluminum blocks. During the tests, load, crosshead position, and time were recorded by the MTS software. The peak force in the load cycle was taken to be the pull-apart force.

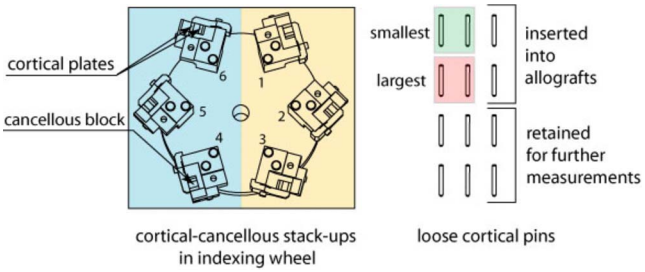

Fig. 4 Depiction of part sorting for one donor. The cortical plate hole diameters for the cortical plate-cancellous block stack ups were measured in the fixture at all locations (1–6). The stack ups in locations 1–3 were left in the fixture and later assembled. For locations 4–6, the plates and blocks were removed and the loose plates remeasured at each subsequent step in the manufacturing process.

Of the 30 assembled allografts, 20 were pulled apart during mechanical testing. For the remaining ten grafts, the epoxy holding the graft to the aluminum blocks failed prior to the interference fit. The average pull-apart force for the 20 successful tests was 83.4 N with a standard deviation of 25.9 N. Of the 20 separated grafts, only 7 exhibited no signs of cracking. The average pull-apart force of the grafts with no cracks was 100.6 N with a standard deviation of 28.5 N. The average pull-apart force of the grafts that exhibited cracks was 74.1 N with a standard deviation of 19.8 N. It should be noted that grafts exhibiting visible cracks are often scrapped by the manufacturer at a loss.

In Fig. 8, the pull-apart force for each graft is compared to the predicted diametral interference determined from the CMM mea-

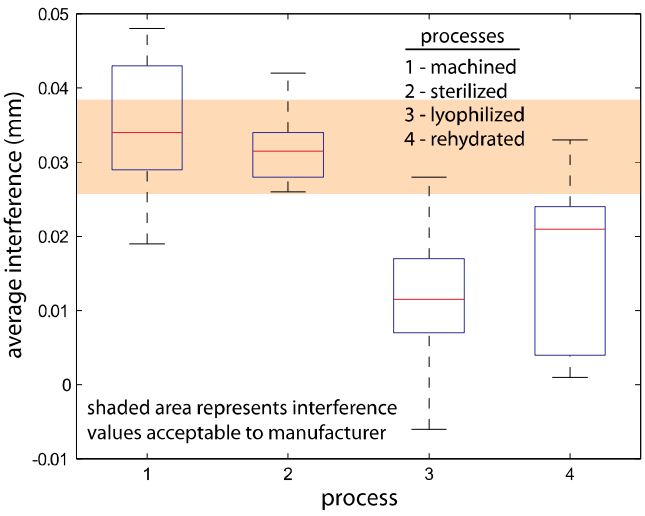

Fig. 5 Box plots of average diametric interference data for each of ten donors as a function of production process

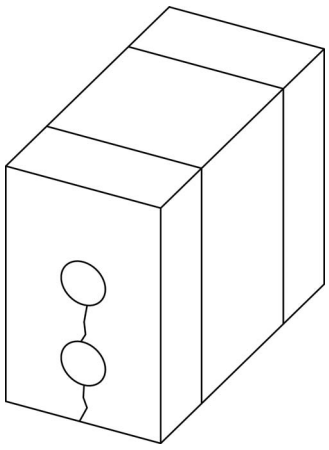

Fig. 6 Illustration of cortical plate cracks

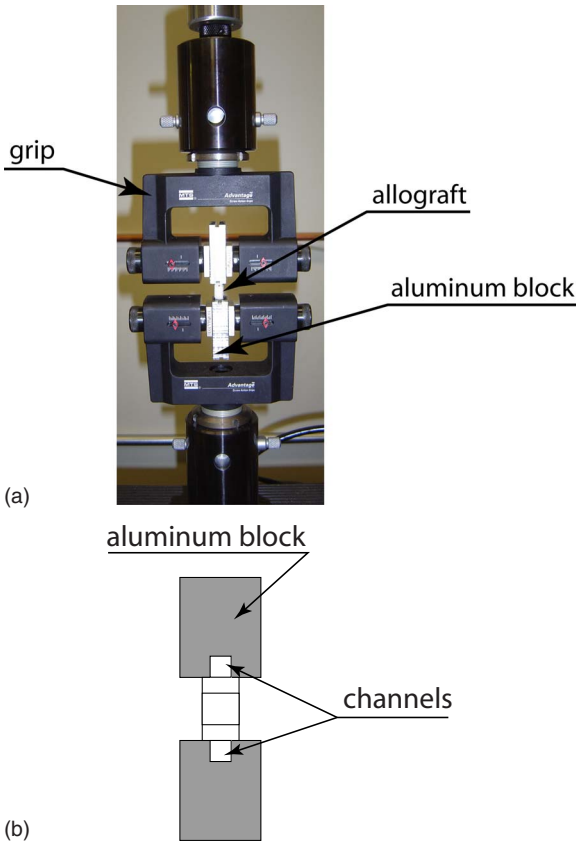

Fig. 7 Pull-apart test setup: (*a*) load frame grips, aluminum holding blocks, and allograft; (*b*) schematic of aluminum blocks epoxied to allograft

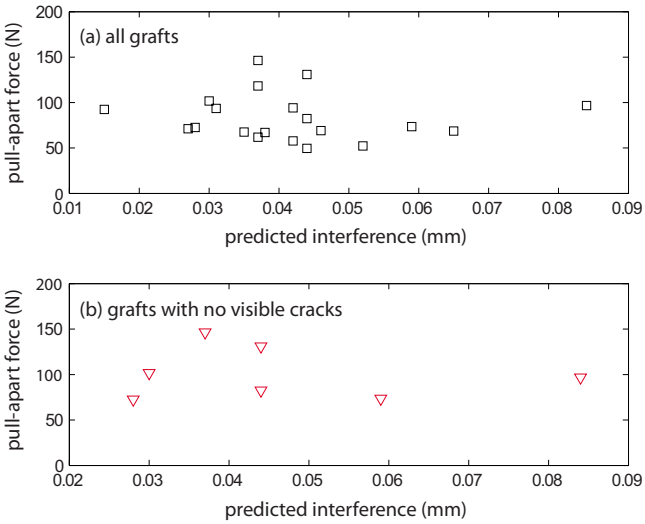

Fig. 8 Pull-apart force versus predicted interference for (*a*) all assembled grafts and (*b*) grafts without cracks

Table 1 Finite element input values for three trials

Property	Trial 1	Trial 2	Trial 3
Young's modulus E_r (GPa)	12.0	12.0	9.0
Young's modulus E_c (GPa)	12.0	12.0	9.0
Young's modulus E_l (GPa)	18.0	18.0	14.0
Shear modulus G_{rc} (GPa)	3.3	3.3	2.9
Shear modulus G_{rl} (GPa)	3.3	3.3	2.9
Shear modulus G_{cl} (GPa)	3.3	3.3	2.9
Poisson's ratio ν_{rc}	0.50	0.50	0.50
Poisson's ratio ν_{rl}	0.40	0.40	0.40
Poisson's ratio ν_{cl}	0.25	0.25	0.25
Friction coefficient μ	0.29	0.29	0.29
Pin diameter D (mm)	1.948	1.936	1.936
Diametral interference (mm)	0.018	0.011	0.011

surements. Unexpectedly, little or no correlation between the predicted diametric interference and the pull-apart force is observed. This could indicate that, for the small sample size (i.e., the seven grafts that were pulled apart and did not exhibit cracking), variations in material properties obfuscate the effects of dimensional interference. It is also possible that the poor correlation between predicted interference and pull-apart force reflects a difference in the effects of lyophilization and/or hydration on the assembled graft as compared to the measured loose parts.

4 Finite Element Analysis

A finite element model of the interference fit was created to both predict allograft failures and validate/improve the isotropic model to be applied in the Monte Carlo simulation (Sec. 5).

ANSYS 10 (ANSYS Inc, Canonsburg, PA) finite element software was used to create the solid model and mesh as well as to complete the analysis. The diameter of the pin in this model was set equal to the average of all pin diameters from the dimensional study. The diameter of the holes was set equal to the pin diameter minus the average predicted interference value from the dimensional study. Twenty-node brick elements were used to describe the bulk material of the pin and the plate. To simulate the interference fit, contact and target elements were created at the pin-plate interfaces. Although cortical bone is actually orthotropic in nature, it has been shown that little error is introduced by approximating material properties as transversely isotropic [3]. Additionally, while bone material can have behave differently in tension than in compression [4,5], no distinction was made in this study.

A two-step load scenario was applied to evaluate the interference fit. First, the static interference condition was used to determine the stresses in the assembled allograft. Von Mises equivalent stress values and contact pressures were obtained from this load step. The next "load" step was to introduce a relative motion of 100 μm at the contact elements between the pins and holes. The pull-apart force was then determined by summing the z-direction forces (along the pin axis) of all contact elements at the pin-plate interfaces.

The finite element analysis was completed three times with three separate sets of material properties and geometric inputs (Table 1). Here, the subscript r refers to the radial bone direction, c to the circumferential bone direction, and l to the longitudinal bone direction. The von Mises stress, S_v, and pull-apart force, F, results from each trial are provided in Table 2. For the first trial, tensile elastic constants reported by Reilly and Burrstein [4] were used, while the pin diameter and diametric interference were taken from the measurement results after hydration. It should be noted that in any instance where Reilly and Burrstein reported Poisson's ratios greater than 0.5, which is physically impossible, a ratio of 0.5 was used. The second trial used the same material properties as the first trial, but applied geometric values measured after lyophilization. The third trial again used the lyophilized state pin diameter and interference value, but the mechanical properties were reduced by one standard deviation (reported in Ref. [4]) from the values used in the first two trials. Of the three, the third trial (reduced modulus and interference values) shows the closest agreement to the experimental data. Since a tabulated value for the static friction coefficient of self-mated milled cortical bone could not be located, it was obtained experimentally using the linear reciprocating tribometer shown in Fig. 9. While exhaustive testing was not performed, the reported value represents a reasonable estimate of the friction behavior of the bone used in this study.

Table 2 Pull-apart force and maximum von Mises stress results from the finite element analysis trials

Trial	Max. von Mises stress (MPa)	Pull-apart force F (N)
1	80.6	216.0
2	45.0	120.3
3	34.6	93.9

The von Mises stress distribution and contact pressure plot for the third trial are shown in Figs. 10 and 11, respectively. Not surprisingly, the highest stresses are located at the contact and between the two pins. However, no defined stress concentration at the edge of the pin-hole contact is observed.

5 Monte Carlo Simulation

A Monte Carlo simulation was developed for predicting failure rates of the interference fit. The simulation was based on a one-dimensional analytical thick-walled cylinder model (Fig. 12).

5.1 Analytical Model. In this model, Cylinder "1" of nominal outer radius R is forced into another hollow Cylinder "2" whose inner radius is $\delta/2$ smaller than R. To accommodate the radial interference, both cylinders must deform such that the outer diameter of Cylinder 1 decreases by some amount δ_1 while the inner diameter of Cylinder 2 increases by some amount δ_2. The deformations δ_1 and δ_2 must sum to the diametral mismatch δ.

The state of stress at the interference fit is determined from this boundary condition and the requirement that the pressure on the outer and inner cylinders be equal at the interface. The interference pressure and maximum von Mises stress for both cylinders is then found using Eqs. (1)–(3) derived from thick-walled cylinder theory [6,7]. Based on these calculations, any von Mises stress S_v in either cylinder, which was greater than the material failure strength, was deemed a failed interference fit. In these equations,

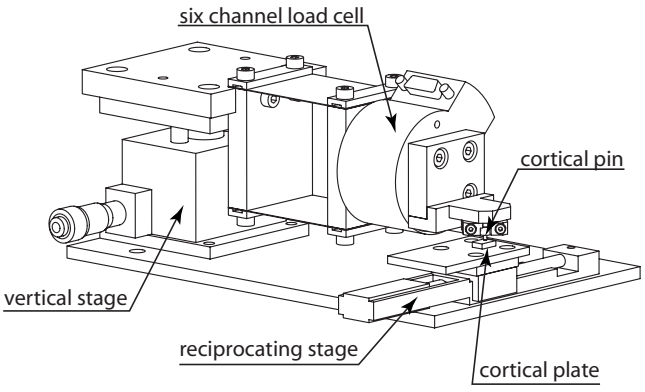

Fig. 9 Reciprocating tribometer used to obtain friction coefficient of self-mated machined cortical bone

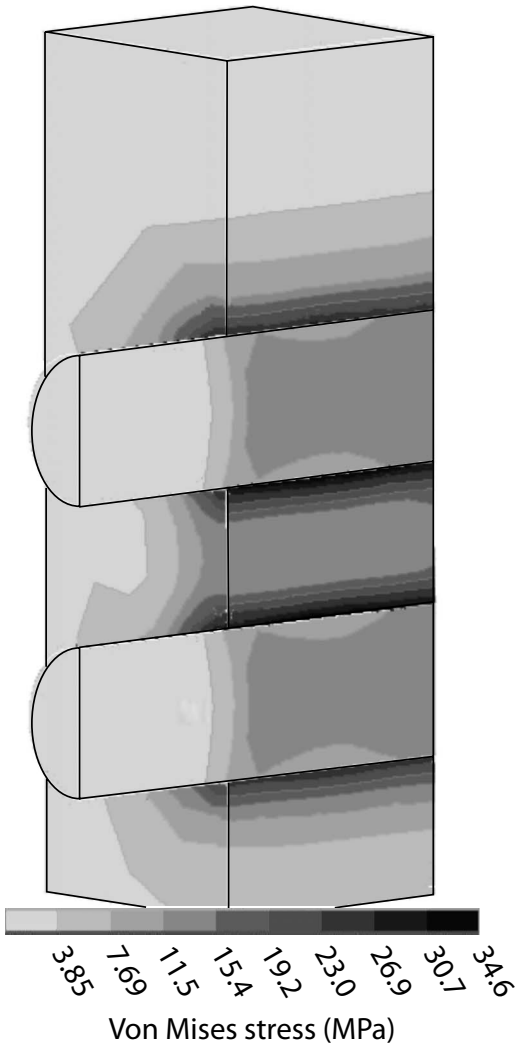

Fig. 10 Sectioned view of von Mises stress distribution predicted by the finite element analysis

K_t is a stress concentration factor that accounts for the fact that neither cylinder was infinitely long. The elastic modulus and Poisson's ratio are represented by E_i and ν_i, respectively, for the two cylinders.

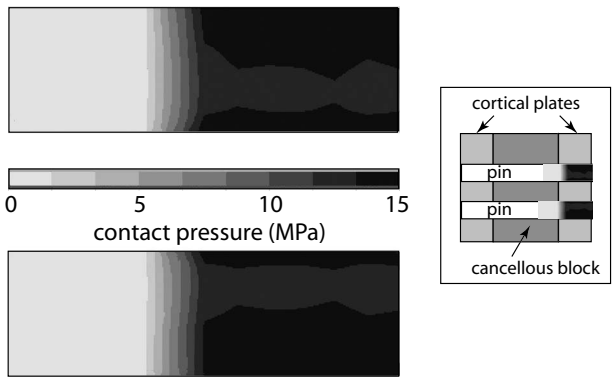

Fig. 11 Contact pressure distribution over portion of a single cortical pin in contact. The *z* direction represents the axial direction of the pin. The inset shows the position of the plot in the allograft.

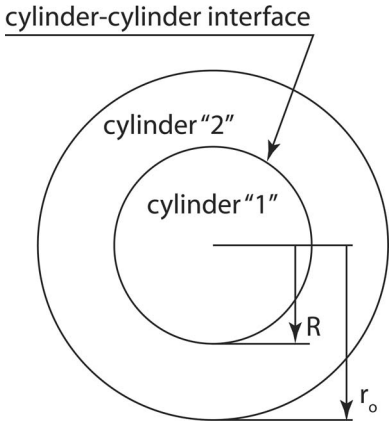

Fig. 12 One-dimensional analytical interference fit model used in the Monte Carlo simulations

$$p = \frac{\delta}{\frac{R}{E_1}(1-\nu_1) + \frac{R}{E_1}\left(\frac{r_o^2+R^2}{r_o^2-R^2}+\nu_2\right)} \tag{1}$$

$$S_{\nu 1} = p\sqrt{K_t^2 - K_t + 1} \tag{2}$$

$$S_{\nu 2} = p\sqrt{K_t^2 - K_t\left(\frac{r_o^2+R^2}{r_o^2-R^2}\right) + \left(\frac{r_o^2+R^2}{r_o^2-R^2}\right)} \tag{3}$$

The force required to separate the interference fit was found by integrating the product of the contact pressure, contact area A_c, and coefficient of friction μ over the axial contact length L_c (Eq. (4)). Failure of the interference fit was assumed to occur for any iteration where the pull-apart force was less than or equal to zero or a von Mises stress was found to be greater than a representative failure stress of 53 MPa [8].

$$F = \int_0^{Lc} \mu K_t(z) \cdot p \cdot (A_c) dz = \int_0^{Lc} \mu K_t(z) p (2\pi R L_c) dz \tag{4}$$

The model described by Eqs. (1)–(4) has three primary limitations for application to the allograft interference fit. First, the model assumes that the material properties of both the pin and plate are isotropic, while bone is not. Second, the model does not account for the effect of the closely spaced second pin on the stress state. Finally, the model assumes that both components will be cylindrical, which is not the case for the two-hole cortical plates used in this study. In other words, the outer radius r_o has no physical meaning for the allograft. To address the latter issue, the r_o term was used as a fitting factor based on the results of the finite element analysis. Despite these concerns, the analytical model was used due to its computational simplicity. Another possible shortcoming is inadequate knowledge of the effective coefficient of friction at the interface, particularly following the postassembly manufacturing processes.

5.2 Simulation Procedures. In Monte Carlo simulation, input parameters are selected randomly from normal distributions and output values are calculated by propagating these individual sets of input parameters through the selected model. This process is repeated many times to obtain the resulting distribution in output values.

Average values and standard deviations of the input parameters selected for this study are given in Table 3. Geometric and elasticity terms are identical to those used in the third finite element study. Note that the stress concentration was set equal to unity based on the results of the finite element analyses.

The Monte Carlo simulation was completed in two formats. In

Table 3 Monte Carlo simulation input parameters and variations (normal distributions were assumed)

Parameter	Mean value	Standard deviation
Diametral interference δ (μm)[a]	11	9
Pin Young's modulus E_1 (GPa) [4]	9	1
Plate Young's modulus E_2 (GPa) [4]	9	1
Pin Poisson's ratio ν_1 [4]	0.41	0.15
Plate Poisson's ratio ν_1 [4]	0.41	0.15
Pin diameter d (mm)[a]	1.937	0.021
Fitting factor r_o (mm)[b]	1.2	0
Stress concentration factor	1	0
Contact length L_c (mm)[a]	7.0	0.3
Coefficient of friction μ[c]	0.29	0.15

[a]Data taken from dimensional measurements.
[b]Set such that simulation mean pull-out force was representative of the finite element analysis results.
[c]Experimentally observed, see Sec. 4.

Table 4 Standard deviations of the single parameter Monte Carlo simulations

Individual parameters	σ_F (N)	Pin σ_{S_v} (MPa)	Plate σ_{S_v} (MPa)
Diametric interference	109	7	38
Coefficient of friction	66	<1	0
Plate Young's modulus	13	1	5
Pin diameter	6	1	1
Contact length	6	1	<1
Pin Poisson's ratio	4	<1	2
Plate Poisson's ratio	4	<1	2

the first, all input parameters were randomly varied as previously discussed to obtain the distribution of plate and pin von Mises stresses and pull-apart force. In the second, individual simulations were performed for each input variable where all other inputs were held constant at their mean value. In this way, the relative influence of each input parameter on the outputs could be observed. All simulations included 2.5×10^5 iterations. Furthermore, von Mises stress was only calculated when the pull-apart force was positive, since it is undefined if no interference is present.

The statistical distributions obtained from the multiple parameter Monte Carlo simulation (first format) is shown in Fig. 13. Thirteen percent of the simulations resulted in zero pull-apart force (negative interference), which agrees with the results seen during manual pull-apart tests. Of the remaining 87% of the iterations where a positive force was predicted, the average pull-apart force was 160 N. The overall standard deviation of the pull-apart forces was 141 N. The mean von Mises stress in the cortical plates was 65 MPa with a standard deviation of 39 MPa. Fifty-seven percent of the iterations resulted in a von Mises value greater than the representative 53 MPa failure stress of cortical bone. Again, this corresponds closely to the frequency of cracks observed in the completed allografts. Finally, the mean von Mises stress in the cortical pins was 12 MPa with a standard deviation of 7 MPa.

Results from the single parameter variation Monte Carlo study are provided in Table 4. The table shows the resulting data spread (represented by one standard deviation, σ) in pull-apart force and von Mises stress in the pin and plate due to the selected variations in the individual input parameters. The simulation indicates that the diametral interference, coefficient of friction, and plate Young's modulus are the most influential parameters for pull-apart

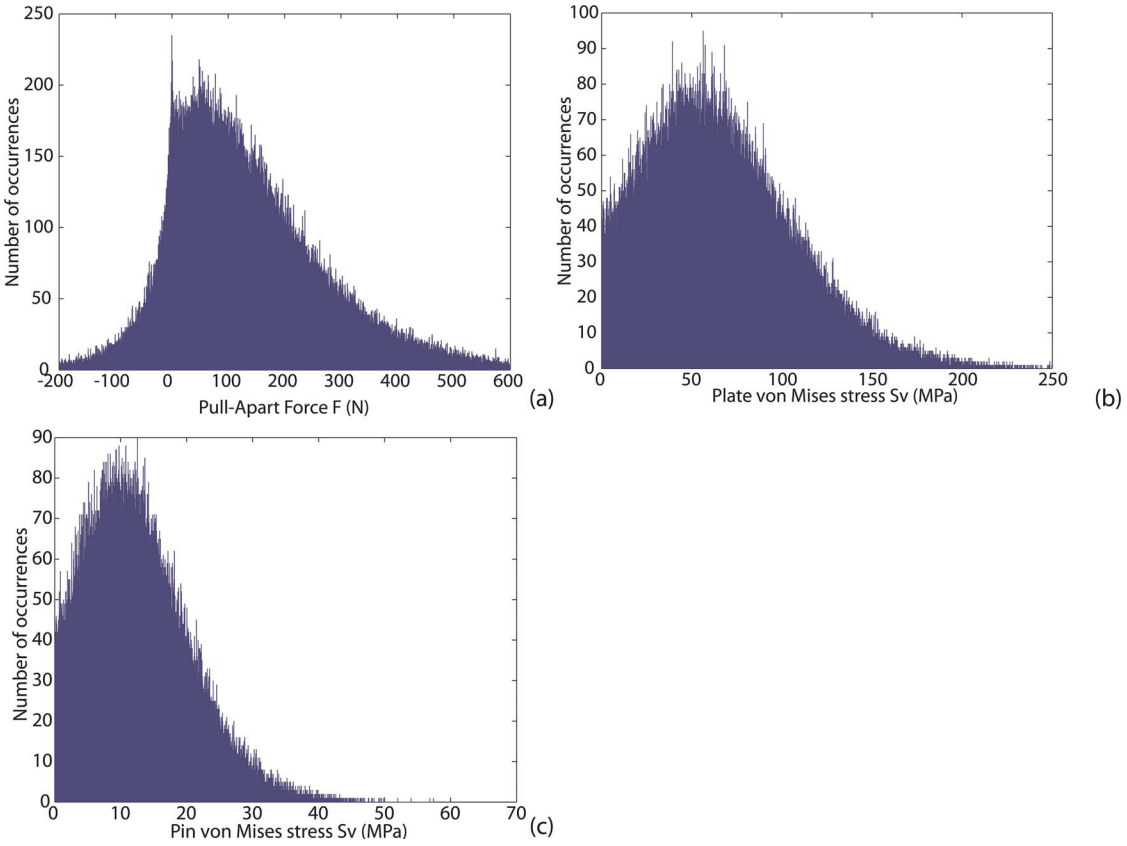

Fig. 13 Statistical distributions of the output parameters from the multiple parameter Monte Carlo simulation: (*a*) pull-apart force; (*b*) von Mises stress in the plate; and (*c*) von Mises stress in the pin

force. Also, the diametral interference, plate Young's modulus, and Poisson's ratio are the most influential factors on the cortical plate von Mises stress.

6 Conclusions

This paper presents the results of a study of interference pin connections in a cortical-cancellous allograft used in spinal fusions. A dimensional study of the interference fit components after several key manufacturing steps indicated that lyophilization, or freeze drying, had the largest influence on component dimension and introduced the largest amount of dimensional variability. Additional insight could be provided by future study of the effects of lyophilization on the dimensions and material properties of the bone material inside the assembled grafts.

The strength of the interference fit was investigated through mechanical tensile tests. While no correlation was observed between the predicted dimensional interference and the strength of the fit, the authors believe that some relationship does exist but was confounded by variations in material properties and process treatments as well as the presence of cracks in the grafts. Further investigation is required to determine how and when these cracks develop and propagate.

A finite element model was created to describe the interference fit, which was able to reasonably predict the average pull-apart strength of the graft. The model predicted the maximum von Mises stress in the graft to be between 34.6 MPa and 80.6 MPa. Additionally, an analytical model of the interference fit was solved within a Monte Carlo simulation. The simulation predicted that diametric interference, coefficient of friction, and the plate modulus are the most influential factors on the interference fit pull-apart force. The simulation also predicted that diametric interference and elastic properties are the most influential factors affecting the cortical plate stress state. Despite limitations of the analytical model, the Monte Carlo simulation accurately reflected the frequency of occurrence of pull-apart and cracking failures at 13% and 57%, respectively.

Acknowledgment

The authors acknowledge helpful discussions with W.G. Sawyer, University of Florida.

References

[1] Huang, P., Gupta, C., Sarigul-Klijn, N., and Hazelwood, S., 2006, "Two In Vivo Surgical Approches for Lumbar Corpectomy Using Allograft and a Metallic Implant: A Controlled Clinical and Biomechanical Study," The Spine Journal, **6**, pp. 648–658.

[2] Komotar, R., Mocco, J., and Kaiser, M., 2006, "Surgical Management of Cervical Myelopathy: Indications and Techniques for Laminectomy and Fusion," The Spine Journal, **6**, pp. 252S–267S.

[3] Huiskes, R., 1982, "On the Modeling of Long Bones in Structural Analyses," J. Biomech., **15**(1), pp. 65–69.

[4] Reilly, D., and Burstein, A., 1975, "The Elastic Modulus and Ultimate Properties of Compact Bone Tissue," J. Biomech., **8**(6), pp. 393–396.

[5] Yoon, H., and Katz, J., 1976, "Ultrasonic Wave Propagation in Human Cortical Bone II: Measurements of Elastic Properties and Micro-Hardness," J. Biomech., **9**, pp. 459–462.

[6] Shigley, J., and Mischke, C., 2001, *Mechanical Engineering Design*, McGraw-Hill, New York.

[7] Boresi, A., and Schmidt, R., 2003, *Advanced Mechanics of Materials*, Wiley, Hoboken, NJ.

[8] Bianchi, J., 1999, "Design and Mechanical Behavior of the MD Series of Bone Dowels," University of Florida, Gainesville, FL, Doctor of Philosophy.